



International Agreement Report

Assessment of TRACE 5.0 Against ROSA-2 Test 3 Counterpart Test to PKL

Prepared by:

S. Gallardo, A. Querol, M. Lorduy, and
G. Verdu

Universitat Politècnica de València
Instituto Universitario de Seguridad Industrial, Radiofísica y Medioambiental
Camí de Vera s/n
46022 Valencia, SPAIN

Kirk Tien, NRC Project Manager

**Division of Systems Analysis
Office of Nuclear Regulatory Research
U.S. Nuclear Regulatory Commission
Washington, DC 20555-0001**

Manuscript Completed: April 2018

Date Published: March 2019

**Published by
U.S. Nuclear Regulatory Commission**

AVAILABILITY OF REFERENCE MATERIALS IN NRC PUBLICATIONS

NRC Reference Material

As of November 1999, you may electronically access NUREG-series publications and other NRC records at NRC's Library at www.nrc.gov/reading-rm.html. Publicly released records include, to name a few, NUREG-series publications; *Federal Register* notices; applicant, licensee, and vendor documents and correspondence; NRC correspondence and internal memoranda; bulletins and information notices; inspection and investigative reports; licensee event reports; and Commission papers and their attachments.

NRC publications in the NUREG series, NRC regulations, and Title 10, "Energy," in the *Code of Federal Regulations* may also be purchased from one of these two sources.

1. The Superintendent of Documents

U.S. Government Publishing Office
Mail Stop IDCC
Washington, DC 20402-0001
Internet: bookstore.gpo.gov
Telephone: (202) 512-1800
Fax: (202) 512-2104

2. The National Technical Information Service

5301 Shawnee Road
Alexandria, VA 22312-0002
www.ntis.gov
1-800-553-6847 or, locally, (703) 605-6000

A single copy of each NRC draft report for comment is available free, to the extent of supply, upon written request as follows:

Address: **U.S. Nuclear Regulatory Commission**
Office of Administration
Multimedia, Graphics, and Storage &
Distribution Branch
Washington, DC 20555-0001
E-mail: distribution.resource@nrc.gov
Facsimile: (301) 415-2289

Some publications in the NUREG series that are posted at NRC's Web site address www.nrc.gov/reading-rm/doc-collections/nuregs are updated periodically and may differ from the last printed version. Although references to material found on a Web site bear the date the material was accessed, the material available on the date cited may subsequently be removed from the site.

Non-NRC Reference Material

Documents available from public and special technical libraries include all open literature items, such as books, journal articles, transactions, *Federal Register* notices, Federal and State legislation, and congressional reports. Such documents as theses, dissertations, foreign reports and translations, and non-NRC conference proceedings may be purchased from their sponsoring organization.

Copies of industry codes and standards used in a substantive manner in the NRC regulatory process are maintained at—

The NRC Technical Library

Two White Flint North
11545 Rockville Pike
Rockville, MD 20852-2738

These standards are available in the library for reference use by the public. Codes and standards are usually copyrighted and may be purchased from the originating organization or, if they are American National Standards, from—

American National Standards Institute

11 West 42nd Street
New York, NY 10036-8002
www.ansi.org
(212) 642-4900

Legally binding regulatory requirements are stated only in laws; NRC regulations; licenses, including technical specifications; or orders, not in NUREG-series publications. The views expressed in contractor prepared publications in this series are not necessarily those of the NRC.

The NUREG series comprises (1) technical and administrative reports and books prepared by the staff (NUREG-XXXX) or agency contractors (NUREG/CR-XXXX), (2) proceedings of conferences (NUREG/CP-XXXX), (3) reports resulting from international agreements (NUREG/IA-XXXX), (4) brochures (NUREG/BR-XXXX), and (5) compilations of legal decisions and orders of the Commission and Atomic and Safety Licensing Boards and of Directors' decisions under Section 2.206 of NRC's regulations (NUREG-0750).

DISCLAIMER: This report was prepared under an international cooperative agreement for the exchange of technical information. Neither the U.S. Government nor any agency thereof, nor any employee, makes any warranty, expressed or implied, or assumes any legal liability or responsibility for any third party's use, or the results of such use, of any information, apparatus, product or process disclosed in this publication, or represents that its use by such third party would not infringe privately owned rights.



International Agreement Report

Assessment of TRACE 5.0 Against ROSA-2 Test 3 Counterpart Test to PKL

Prepared by:
S. Gallardo, A. Querol, M. Lorduy, and
G. Verdu

Universitat Politècnica de València
Instituto Universitario de Seguridad Industrial, Radiofísica y Medioambiental
Camí de Vera s/n
46022 Valencia, SPAIN

Kirk Tien, NRC Project Manager

**Division of Systems Analysis
Office of Nuclear Regulatory Research
U.S. Nuclear Regulatory Commission
Washington, DC 20555-0001**

Manuscript Completed: April 2018
Date Published: March 2019

**Published by
U.S. Nuclear Regulatory Commission**

ABSTRACT

The purpose of this work is to overview the results obtained by the simulation of the Counterpart Test 3 PKL-ROSA (SB-HL-18 in JAEA) in the Large Scale Test Facility (LSTF) using the thermal-hydraulic code TRACE5 patch 2. This experiment simulates a PWR hot leg Small Break Loss-Of-Coolant Accident (SBLOCA).

One of the main objectives of this test is to establish a relationship between the Core Exit Temperature (CET) measured by the thermocouples and the fuel rod surface temperature (Peak Cladding Temperature, PCT). The core exit thermocouples are used as an important indicator to start an accident management (AM) operator action by detecting core temperature excursion during reactor accidents. Test 3 provides experimental data to study the relation between CET and PCT and the time delay existing between them.

A detailed model of the LSTF and the control logic of the Test 3 have been simulated using TRACE5 patch 2. The main thermal hydraulic variables obtained with TRACE5 have been compared with experimental data. In general, the simulation results are able to reproduce the experimental behavior.

FOREWORD

Thermalhydraulic studies play a key role in nuclear safety. Important areas where the significance and relevance of TH knowledge, data bases, methods and tools maintain an essential prominence are among others:

- assessment of plant modifications (e.g., Technical Specifications, power uprates, etc.);
- analysis of actual transients, incidents and/or start-up tests;
- development and verification of Emergency Operating Procedures;
- providing some elements for the Probabilistic Safety Assessments (e.g., success criteria and available time for manual actions, and sequence delineation) and its applications within the risk informed regulation framework;
- training personnel (e.g., full scope and engineering simulators); and/or
- assessment of new designs.

For that reason, the history of the involvement in Thermalhydraulics of CSN, nuclear Spanish Industry as well as Spanish universities, is long. It dates back to mid 80's when the first serious talks about Spain participation in LOFT-OCDE and ICAP Programs took place. Since then, CSN has paved a long way through several periods of CAMP programs, promoting coordinated joint efforts with Spanish organizations within different periods of associated national programs (i.e., CAMP-España).

From the CSN perspective, we have largely achieved the objectives. Models of our plants are in place, and an infrastructure of national TH experts, models, complementary tools, as well as an ample set of applications, have been created. The main task now is to maintain the expertise, to consolidate it and to update the experience. We at the CSN are aware on the need of maintaining key infrastructures and expertise, and see CAMP program as a good and well consolidated example of international collaborative action implementing recommendations on this issue.

Many experimental facilities have contributed to the today's availability of a large thermal-hydraulic database (both separated and integral effect tests). However there is a continuous need for additional experimental work and code development and verification, in areas where no emphasis have been made along the past. On the basis of the SESAR/FAP¹ reports "*Nuclear Safety Research in OECD Countries: Major Facilities and Programmes at Risk*" (SESAR/FAP, 2001) and its 2007 updated version "*Support Facilities for Existing and Advanced Reactors (SFEAR) NEA/CSNI/R(2007)6*", CSNI is promoting since the beginning of this century several collaborative international actions in the area of experimental TH research. These reports presented some findings and recommendations to the CSNI, to sustain an adequate level of research, identifying a number of experimental facilities and programmes of potential interest for present or future international collaboration within the nuclear safety community during the coming decade. The different series of PKL, ROSA and ATLAS projects are under these premises.

CSN, as Spanish representative in CSNI, is involved in some of these research activities, helping in this international support of facilities and in the establishment of a large network of international collaborations. In the TH framework, most of these actions are either covering not

¹ SESAR/FAP is the Senior Group of Experts on Nuclear Safety Research Facilities and Programmes of NEA Committee on the Safety of Nuclear Installations (CSNI).

enough investigated safety issues and phenomena (e.g., boron dilution, low power and shutdown conditions, beyond design accidents), or enlarging code validation and qualification data bases incorporating new information (e.g., multi-dimensional aspects, non-condensable gas effects, passive components).

This NUREG/IA report is part of the Spanish contribution to CAMP focused on:

- Analysis, simulation and investigation of specific safety aspects of PKL2/OECD and ROSA2/OECD experiments.
- Analysis of applicability and/or extension of the results and knowledge acquired in these projects to the safety, operation or availability of the Spanish nuclear power plants.

Both objectives are carried out by simulating the experiments and conducting the plant application with the last available versions of NRC TH codes (RELAP5 and/or TRACE). On the whole, CSN is seeking to assure and to maintain the capability of the national groups with experience in the thermalhydraulics analysis of accidents in the Spanish nuclear power plants. Nuclear safety needs have not decreased as the nuclear share of the nations grid is expected to be maintained if not increased during next years, with new plants in some countries, but also with older plants of higher power in most of the countries. This is the challenge that will require new ideas and a continued effort.

Rosario Velasco García, CSN Vice-president
Nuclear Safety Council (CSN) of Spain

TABLE OF CONTENTS

ABSTRACT	iii
FOREWORD.....	v
LIST OF FIGURES.....	ix
LIST OF TABLES.....	xi
EXECUTIVE SUMMARY.....	xiii
ACKNOWLEDGMENTS	xv
ABBREVIATIONS AND ACRONYMS	xvii
1 INTRODUCTION	1
2 LSTF FACILITY DESCRIPTION.....	3
3 TRANSIENT DESCRIPTION	5
4 TRACE5 MODEL OF LSTF	9
5 RESULTS AND DISCUSSION	13
5.1 Steady-State	13
5.2 Transient	14
5.3 System Pressures	15
5.4 Break.....	16
5.5 Primary Loop Mass Flows	17
5.6 Vessel Collapsed Liquid Levels	19
5.7 Maximum Fuel Rod Surface and Core Exit Temperatures	22
5.8 Hot and Cold Legs Liquid Levels	23
5.9 Emergency Core Cooling Systems Mass Flow Rates	26
5.10 Core Power	28
5.11 Void Fraction	28
6 CONCLUSIONS	35
7 REFERENCES	37

LIST OF FIGURES

Figure 1	Schematic View of the LSTF Facility	3
Figure 2	Model Nodalization.....	10
Figure 3	Primary and Secondary Pressures	16
Figure 4	Break Mass Flow Rate	17
Figure 5	Primary Loop A Mass Flow Rate.	18
Figure 6	Primary Loop B Mass Flow Rate.	18
Figure 7	Core Collapsed Liquid Level.....	19
Figure 8	Upper Plenum Collapsed Liquid Level.....	20
Figure 9	Downcomer Collapsed Liquid Level	21
Figure 10	Fuel Rod Surface Temperatures at Different Axial Positions.	22
Figure 11	Maximum Fuel Rod Surface Temperature vs Core Exit Temperature.....	23
Figure 12	Collapsed Liquid Level in the Hot Leg A.....	24
Figure 13	Collapsed Liquid Level in the Hot Leg B.....	24
Figure 14	Collapsed Liquid Level in the Cold Leg A.....	25
Figure 15	Collapsed Liquid Level in the Cold Leg B.....	25
Figure 16	High Pressure Injection System Mass Flow Rate.....	26
Figure 17	Accumulator Injection System Mass Flow Rate.....	27
Figure 18	Low Pressure Injection System Mass Flow Rate.....	27
Figure 19	Core Power	28
Figure 20	Void Fraction in the LSTF at 0 s	29
Figure 21	Void Fraction in the LSTF when PCT Reaches 750 K and HPI Starts.....	30
Figure 22	Void Fraction in the LSTF when Primary Pressure = 5 MPa.....	31
Figure 23	Void Fraction in the LSTF when Second PCT Excursion is Produced	32
Figure 24	Void Fraction in the LSTF at the End of the Transient.....	33

LIST OF TABLES

Table 1	Control Logic and Sequence of Major Events in the Experiment	6
Table 2	Core Protection Logic.....	7
Table 3	Vessel Nodalization.....	9
Table 4	Steady-State Comparison between Experimental and Simulated Values.....	13
Table 5	Sequence of Events Comparison between Experiment and TRACE5..	14

EXECUTIVE SUMMARY

The purpose of this work is to test the capability of the thermal hydraulic code TRACE5 in the simulation of a Hot Leg Small Break LOCA (SBLOCA) in the frame of the OECD/NEA ROSA-2 Project. The main objective of this project is providing experimental data in the Large Scale Test Facility (LSTF) for assessment of thermal hydraulic computer codes. The transient considered in this work, Test 3, reproduces a PWR 1.5% hot leg SBLOCA with an assumption of total failure of High Pressure Injection (HPI) system.

Test 3 was designed as counterpart test between PKL and LSTF test facilities. One of the purposes of this test is to clarify the relation between the Core Exit Temperature (CET) measured by thermocouples and the Peak Cladding Temperature (PCT) at high and low-pressure conditions corresponding to the pressure range of LSTF and PKL facilities during a hot leg SBLOCA.

TRACE5 patch 2 has been used to model the LSTF and the control logic of Test 3. The model considers the high-pressure phase, the conditioning phase and the low-pressure phase performed in the LSTF experiment.

The behavior of the Pressure Vessel is analyzed, measuring the active core, upper plenum, upper head and downcomer liquid levels. Results of the simulation with TRACE5 are compared with the experimental measurements in several graphs, including primary and secondary pressures, break mass flow rate, primary mass flow rates, and collapsed liquid levels (hot leg, steam generators U-tubes, etc.).

ACKNOWLEDGMENTS

This paper contains findings that were produced within the OECD-NEA ROSA-2 Project. The authors are grateful to the Management Board of the ROSA Project for their consent to this publication, and thank the Spanish Nuclear Regulatory Body (CSN) for the technical and financial support under the agreement STN/1388/05/748.

ABBREVIATIONS AND ACRONYMS

AFW	Auxiliary Feedwater
AIS	Accumulator Injection System
AM	Accident Management
BE	Best Estimate
CAMP	Code Assessment and Management Program
CET	Core Exit Temperature
CPU	Central Processing Unit
CRGT	Control Rod Guide Tubes
CSN	Nuclear Safety Council, Spain
DBE	Design Basis Event
ECCS	Emergency Core Cooling System
HPI	High Pressure Injection
IBLOCA	Intermediate Break Loss-Of-Coolant Accident
JAEA	Japan Atomic Energy Agency
JAERI	Japan Atomic Energy Research Institute
JC	Jet Condenser
LOCA	Loss-Of-Coolant Accident
LPI	Low Pressure Injection
LSTF	Large Scale Test Facility
MFW	Main Feedwater
MSIV	Main Steam Isolation Valve
NPP	Nuclear Power Plant
NRC	U.S. Nuclear Regulatory Commission
NV	Normalized to the Steady State Value
PA	Auxiliary Feedwater Pump
PCT	Peak Cladding Temperature
PF	Feedwater Pump
PGIT	Primary Gravity Injection Tank
PJ	High Pressure Charging Pump
PL	High Pressure Injection Pump
PV	Pressure Vessel
PWR	Pressurized Water Reactor
PZR	Pressurizer
RHR	Residual Heat Removal
RV	Relief Valve
SBLOCA	Small Break Loss-Of-Coolant Accident
SG	Steam Generator
SI	Safety Injection
SNAP	Symbolic Nuclear Analysis Package
SRV	Safety Relief Valve
ST	Storage Tank

1 INTRODUCTION

The purpose of this work is to describe the most relevant results achieved by using the thermal hydraulic code TRACE5 patch 2 [1, 2] to simulate the SBLOCA transient defined in Test 3 within the OECD/NEA ROSA-2 Project (SB-HL-18 in JAEA) [3]. This transient was performed in the Large Scale Test Facility (LSTF) [4], which simulates a PWR reactor, Westinghouse type, of four loops and 3423 MW of thermal power, scaled to 1/48 in volume and two loops.

Thermocouples are commonly used as an important indicator to start an Accident Management (AM) action by detecting the Core Exit Temperature (CET) excursion during reactor accidents. However, in some tests, a time delay between the detection of superheated steam by thermocouples and the CET excursion is observed [5, 6, 7]. The CET reliability to detect core uncover during a SBLOCA is considered as one of the most important safety concerns studied in the ROSA-2 Project.

Test 3 was designed as counterpart test between the PKL and LSTF test facilities. One of the purposes of this test is to clarify the relation between the CET measured by thermocouples and the fuel rod surface temperature (PCT) at high and low-pressure conditions corresponding to the pressure range of LSTF and PKL facilities during a hot leg SBLOCA. Another goal of this counterpart test is to study two large integral test facilities with different designs to draw technical findings useful for solving scaling problems.

2 LSTF FACILITY DESCRIPTION

In this section, a brief description of the LSTF facility [10] is presented. LSTF simulates a PWR reactor, Westinghouse type, of four loops and 3423 MW of thermal power. The facility is electrically heated, scaled 1:1 in height and 1:48 in flow areas and volumes, with exception of the loops, which are defined by a scaling factor of 1:24 in flow areas and volumes. Figure 1 shows the scheme of the LSTF facility. As it can be seen, the primary coolant system consists of the Pressure Vessel (PV) and two symmetrical primary loops: loop A with the pressurizer (PZR) and loop B.

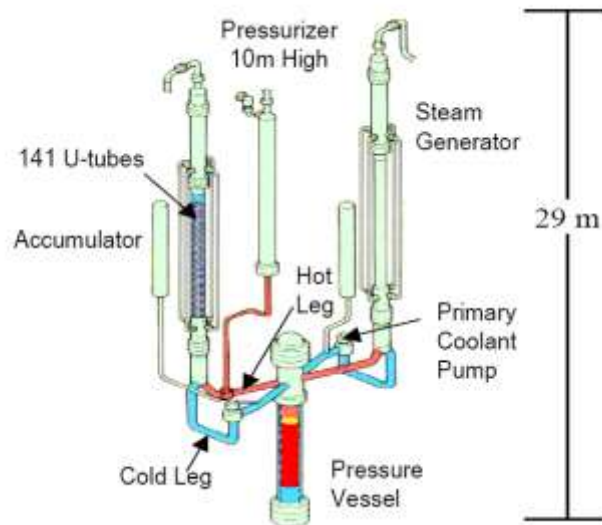


Figure 1 Schematic View of the LSTF Facility

Each loop contains a primary Coolant Pump (PC) and a Steam Generator (SG). The secondary-coolant system consists of the jet condenser (JC), the Feedwater Pump (PF), the Auxiliary Feedwater Pumps (PA) and related piping system in addition to two SG secondary systems.

The Pressure Vessel (PV) is composed of an upper head above the upper core support plate, the upper plenum between the upper core support plate and the upper core plate, the core, the lower plenum and the downcomer annulus region surrounding the core and upper plenum. LSTF vessel has 8 upper head spray nozzles (of 3.4 mm inner-diameter), and 8 Control Rod Guide Tubes (CRGTs) characterize the flow path between the upper head and upper plenum. The maximum core power of the LSTF is limited to 10 MW which corresponds to 14% of the volumetrically scaled PWR core power and is sufficiently capable to simulate PWR decay heat power after the reactor scram.

Regarding the SGs, each of them contains 141 U-tubes which can be classified into separate groups depending on their length. The U-tubes have an inner diameter of 19.6 mm and an outer diameter of 25.4 mm (with 2.9 mm wall thickness). On the other hand, vessel, plenum and riser of steam generators have a height of 19.840, 1.183 and 17.827 m, respectively. The downcomer is 14.101 m in height.

3 TRANSIENT DESCRIPTION

Test 3 reproduces a PWR hot leg Small Break LOCA, which flow area corresponds to 1.5% of reference PWR cold leg area, with High Pressure Injection (HPI) into the PV upper plenum [3]. The transient performed in LSTF is divided into three phases; high-pressure transient phase, conditioning phase, and low-pressure transient phase to meet the PKL pressure. The complete control logic of the transient is listed in Table 1.

The transient starts at time 0 with opening the break valve in the hot leg of loop without pressurizer and increasing the rotational speed of the coolant pumps. Few seconds afterwards, the scram signal is generated. This signal produces the initiation of the core power decay curve. In addition, the scram signal produces the initiation of the primary coolant pumps coast, the turbine trip, the closure of the Main Steam Isolation Valves (MSIV) and the termination of the Main Feedwater (MFW).

To protect the facility, the LSTF Core Protection System automatically decreases the core power when the maximum fuel rod surface temperature reaches 958 K, as it can be seen in Table 2.

Immediately after the maximum fuel rod surface temperature reaches 750 K, the HPI system injects coolant into the PV upper plenum to avoid subcooled water layer being formed at the PV bottom. This phase is terminated when the primary pressure decreases to 5 MPa and the break valve is temporarily closed.

In the conditioning phase, the core power is manually changed to a constant value (1.16 MW). The primary mass inventory is recovered by the continuous HPI injection into the PV upper plenum. When the hot leg liquid level recovers up to the middle level, the HPI is terminated. The Relief Valves (RVs) are fully opened in both SGs for depressurization. The Auxiliary Feedwater (AFW) is then injected into both SGs to avoid significant liquid level drop. When the primary pressure decreases to 3.9 MPa, the RVs are closed and AFW is terminated in both SGs. This phase is finished when the primary pressure reaches 4.5 MPa.

In the low-pressure phase, the break valve is again opened. Due to the coolant loss through the break, the core uncover is produced. Immediately after the CET reaches 623 K, the SG secondary-side depressurization is initiated by fully opening the RVs at both SG as an AM action. The AFW is also injected into both SGs.

The Accumulator Injection system (AIS) is initiated when the primary pressure reaches 2.6 MPa. The Low Pressure Injection (LPI) system is actuated when the PV lower plenum pressure reaches 1 MPa. The transient is terminated when continuous core cooling by the LPI system is confirmed.

Table 1 Control Logic and Sequence of Major Events in the Experiment

Break.	Time zero	High-pressure transient phase
Generation of scram signal.	Primary pressure = 12.97 MPa	
Pressurizer (PZR) heater off.	Generation of scram signal or PZR liquid level below 2.3 m	
Initiation of core power decay curve.	Generation of scram signal.	
Initiation of Primary Coolant Pump coastdown.	Generation of scram signal.	
Turbine trip (closure of steam generators Main Steam Isolation Valves).	Generation of scram signal.	
Closure of steam generators Main Steam Isolation Valves.	Generation of scram signal.	
Termination of steam generators Main Feedwater.	Generation of scram signal.	
Generation of Safety Injection (SI) signal.	Primary pressure = 12.27 MPa	
Initiation of High Pressure Injection system (HPI) into the pressure vessel upper plenum.	Maximum fuel rod surface temperature = 750 K.	
Initiation of steam generators secondary-side depressurization by fully opening of Relief Valves in both loops as AM action.	Maximum core exit temperature = 623 K	Low-pressure transient phase
Initiation of Auxiliary Feed Water in both loops	Initiation of AM action.	
Initiation of Accumulator Injection system in both loops	Primary pressure = 2.6 MPa	
Termination of Accumulator Injection system in both loops	Primary pressure = 1.2 MPa	
Initiation of Low Pressure Injection system in both loops	PV lower plenum pressure = 1 MPa	

Table 2 Core Protection Logic

Core power to	Maximum fuel rod surface temperature (K)
70%	958 K
35%	961 K
13%	966 K
5%	977 K
0% (core power trip)	1003 K

4 TRACE5 MODEL OF LSTF

LSTF has been modeled with 97 hydraulic components (11 BREAKs, 12 FILLs, 25 PIPEs, 2 PUMPs, 1 PRIZER, 26 TEEs, 19 VALVEs and 1 VESSEL). Figure 2 shows the nodalization of the model using the Symbolic Nuclear Analysis Package software (SNAP) [9].

Primary side comprises cold and hot legs, pumps, loop seals, a pressurizer in loop A, the ECCS which includes AIS, HPI and LPI systems, the U-tubes of both SG and the PV. On the other hand, secondary side includes steam separators, risers, downcomers, Safety Relief Valves, Main Steam Isolation Valves and FILLs to provide Main Feedwater and Auxiliary Feedwater.

The pressure vessel has been modelled using a 3D-VESSEL component. The VESSEL nodalization consists of 20 axial levels, 4 radial rings and 10 azimuthal sectors. For each axial level, volume and effective flow area fractions have been set according to technical specifications provided by the organization [4]. Table 3 shows the vessel nodalization in the axial direction.

Table 3 Vessel Nodalization

Levels	Parts of the vessel
1-2	Lower plenum
3-11	Core
12	Upper core plate
13-16	Upper plenum
17	Upper core support plate
18-20	Upper head

The 3D-VESSEL is connected to different 1D components: 8 Control Rod Guide Tubes (CRGT), hot leg A and B (level 15), cold leg A and B (level 15) and a bypass channel (level 14). The CRGTs have been simulated by PIPE components, connecting levels 14 and 19 and allowing the flow between upper head and upper plenum.

30 HTSTR components simulate the fuel assemblies in the active core. A POWER component manages the power supplied by each HTSTR to the 3D-VESSEL. Fuel elements (1008 in total) were distributed into the 3 rings: 154 elements in ring 1, 356 in ring 2 and 498 in ring 3. In both axial and radial direction, different peaking factors have been considered. The power ratio in the axial direction presents a peaking factor of 1.495, while the radial power profile is divided into three power zones using the first three radial rings. Depending on the radial ring, different peaking factors have been considered (0.66 in ring 1, 1.51 in ring 2 and 1.0 in ring 3). The number of fuel rod components associated with each heat structure has been determined from the technical documentation given, considering the distribution of fuel rod elements in the vessel.

A detailed model of SG (geometry and thermal features) has been developed. Boiler and downcomer components of secondary-side have been modeled by TEE components. U-tubes have been classified into three groups according to each average length.

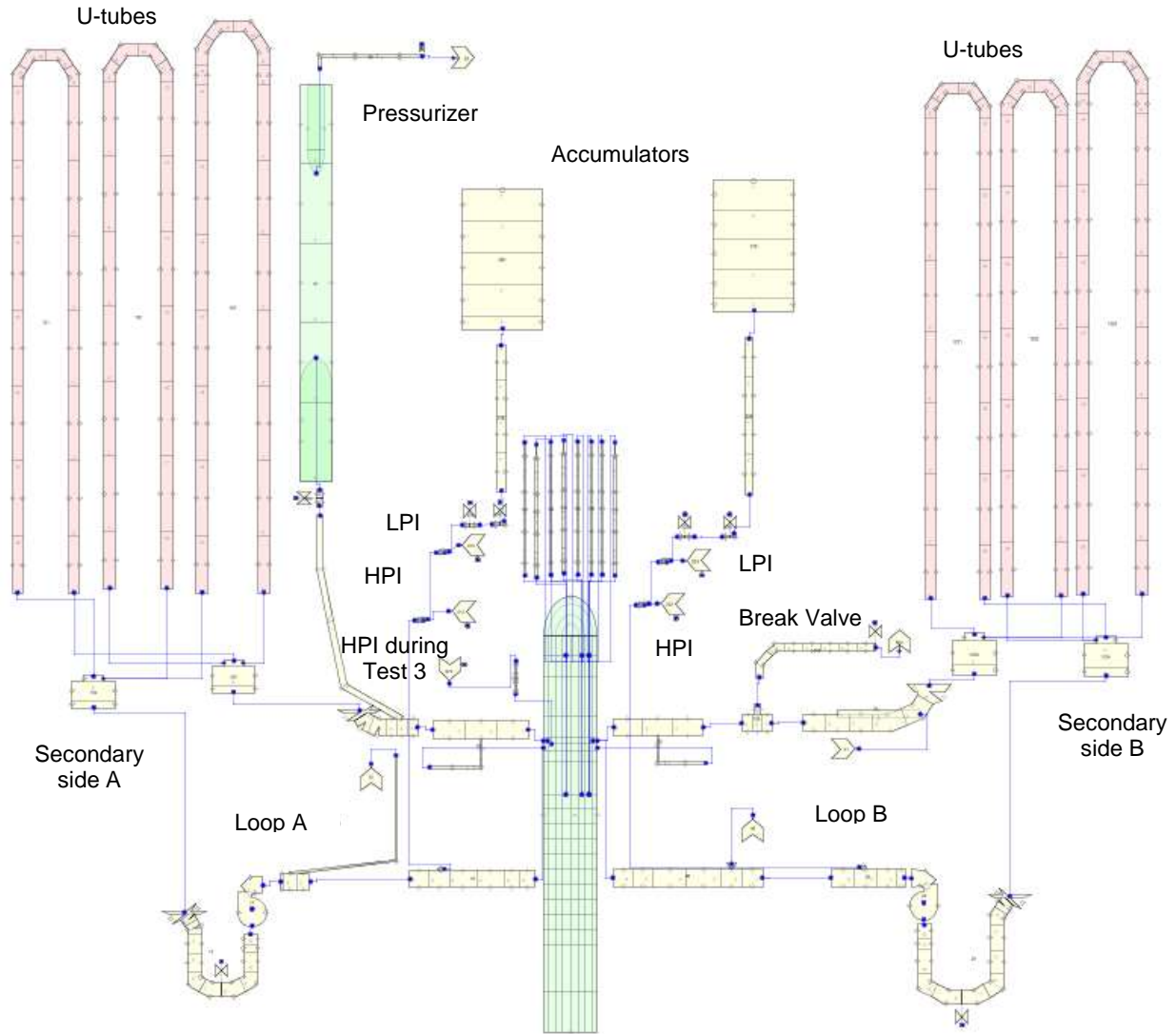


Figure 2 Model Nodalization

The steam separator can be simulated in TRACE5 setting a friction coefficient (FRIC) greater than 10^{22} at a determined cell edge, allowing only gas phase to flow through the cell interface. Heat transfer between primary and secondary sides has been performed using HTSTR components. Cylindrical-shape geometry has been used to best fit heat transmission. Inner and outer surface boundary conditions for each axial level have been set to couple HTSTR component to hydro components (primary and secondary fluids). Different models varying the number of U-tube groups were tested (1, 3 and 6 groups). It was found that the results do not apparently change, using these models. Heat losses to the environment have been considered in the secondary-side walls.

Choke model predicts for a given cell the conditions for which choked flow is expected to occur, providing three different models: subcooled-liquid, two-phase and single-phase vapor model. TRACE5 patch 2 code allows to choose the subcooled-liquid and two-phase coefficients. In this case, the default values (1.0) have been selected. The break has been simulated by means of a VALVE component connected to a BREAK component to establish the boundary conditions.

5 RESULTS AND DISCUSSION

5.1 Steady-State

Steady-state conditions achieved in the simulation were in reasonable agreement with the experimental values. It can be seen in Table 4, where the relative errors (%) between experimental and simulated results for different items are listed. To achieve the steady state conditions, the duration of simulation was stated to 1000 s.

Table 4 Steady-State Condition Comparison between Experimental and Simulated Values

Item (Loop with PZR)	Relative Error (%)
Core Power	0.00
Hot leg Fluid Temperature	0.10
Cold leg Fluid Temperature	0.27
Mass Flow Rate	3.68
Pressurizer Pressure	0.06
Pressurizer Liquid Level	3.60
Accumulator System Pressure	-0.38
Accumulator System Temperature	-0.56
SG Secondary-side Pressure	0.96
SG Secondary-side Liquid Level	5.67
Steam Flow Rate	3.86
Main Feedwater Flow Rate	3.40
Main Feedwater Temperature	0.06
Auxiliary Feedwater Temperature	-0.13

5.2 Transient

Table 5 lists the chronological sequence of the transient events and the comparison between the experiment and TRACE.

Table 5 Chronological Sequence of Events Comparison between Experiment and TRACE5

Event	Experiment Time (s)	TRACE5 Time (s)
Break valve open	0	0
Scram signal	29	32
Closure of steam generators (SG) Main Steam Isolation Valves	32	33
Initiation of coastdown of primary coolant pumps	33	35
Termination of SG main feedwater	34	33
SI signal	37	43
Initiation of core power decay	50	47
Primary coolant pumps stop	281	280
Primary pressure lower than secondary side pressure	1310	1317
The increasing in fuel rod surface temperature starts	1595	1680
Maximum fuel rod surface temperature reached 750 K	1840	1796
Initiation of High Pressure Injection (HPI) into the PV upper plenum	1844	1796
Break valve closure	2172	2113
Manual change of core power to a constant value	2215	2500
Termination of HPI system into the PV upper plenum	2852	2880
Initiation of SG secondary-side depressurization by fully opening Relief Valves (RVs) in both loops	2880	2893
Initiation of Auxiliary Feed Water (AFW) in both loops	2900	2893
Termination of SG secondary-side depressurization	3028	2959
Termination of AFW in both loops	3055	2959
Break valve open again	3323	3303
Start of the increasing in fuel rod surface temperature	3983	4203

Primary pressure becomes lower than SG secondary side pressure	4105	4250
Maximum core exit temperature = 623 K	4390	4507
Initiation of SG secondary-side depressurization by fully opening RVs in both loops as AM action	4394	4519
Initiation of AFW in both loops	4410	4519
Maximum fuel rod surface temperature	4413	4545
Initiation of Accumulator Injection system (AIS) in both loops	4500	4590
Termination of AIS in both loops	4829	4786
Initiation of Low Pressure Injection (LPI) system in both loops	5003	4830

5.3 System Pressures

A comparison between primary and secondary pressures is presented in Figure 3. In the high-pressure phase (until 2100 s), the primary pressure starts to decrease when the break valve is opened due to the coolant discharged through the break. The scram signal is generated when the primary pressure is lower than 12.97 MPa. The SI signal is generated when the primary pressure reaches 12.27 MPa.

The generation of the scram signal causes the closure of SG MSIVs and the beginning of the primary coolant pumps coastdown. The SG secondary-side pressure rapidly increases after the closure of MSIVs. From this moment on, the SG secondary-side pressure starts to oscillate by opening and closing the RVs of both SGs.

The primary pressure becomes lower than the SG secondary-side pressure at about 1250 s soon after the break flow turns into single-phase steam (Figure 4) and decreases until 5 MPa (at 2170 s), when the break valve is closed.

In the conditioning phase (until 3300 s), the primary pressure increases once up to 6.5 MPa and decreases to 4 MPa following the SG secondary-side depressurization. The primary and secondary pressures increase again up to about 4.5 MPa after the termination of the SG secondary-side depressurization.

The low-pressure phase starts by opening the break valve again (at 3300 s). The primary pressure becomes lower than the SG pressure at about 4100 s, slightly after the core boil-off is produced. Immediately after the CET reaches 623 K (Figure 10), the SG secondary-side depressurization is initiated. Then, the primary pressure decreases following the SG pressure and activates the Accumulator Injection and the Low Pressure Injection systems.

In general, both primary and secondary-side pressures are successfully reproduced by TRACE5 in the whole transient. However, some discrepancies are observed regarding the pressure drop slopes, which are different in all the cases.

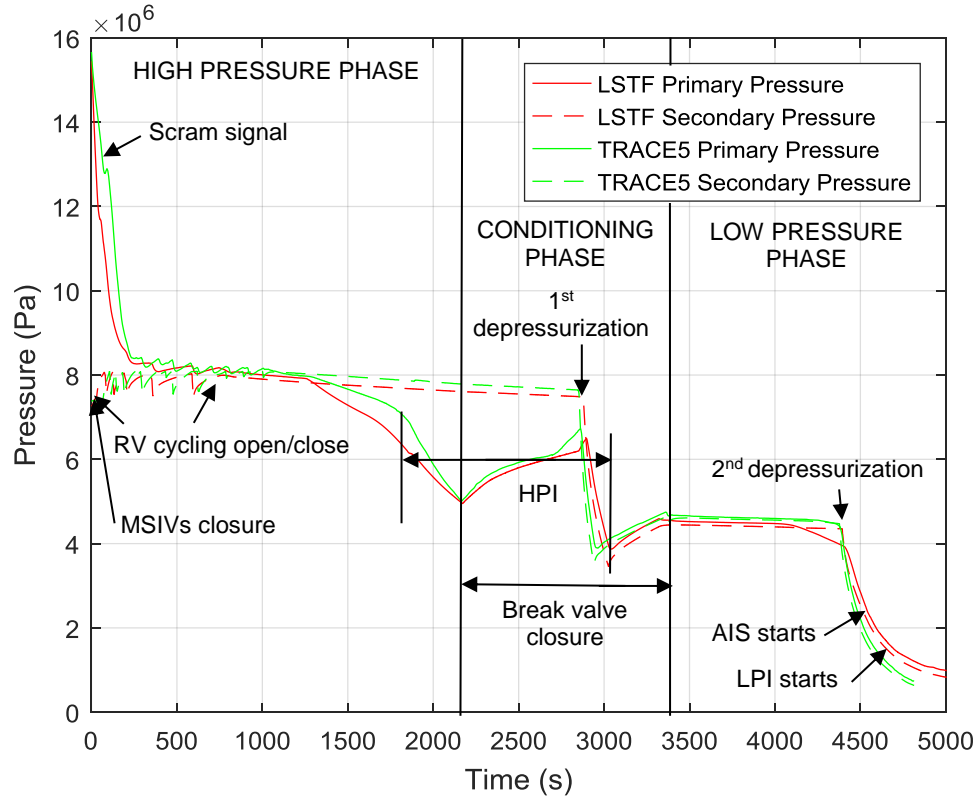


Figure 3 Primary and Secondary Pressures

5.4 Break

Figure 4 shows the mass flow rate through the break. In the high-pressure phase, the break flow rate decreases when the break flow turns from single-phase liquid to two-phase flow (200 s). At 1250 s, the break flow turns to single-phase vapor. To adjust the break mass flow rate with TRACE5, a sensitivity analysis varying the discharge coefficient of the Choked Flow model was performed. In the results shown, the discharge coefficients have been fixed to 1.0.

During the interval between 250 and 1000 s, the mass flow rate through the break obtained with TRACE5 is higher than the experimental values. However, the changes from liquid to two-phase and from two-phase to one phase vapor are reproduced at similar time.

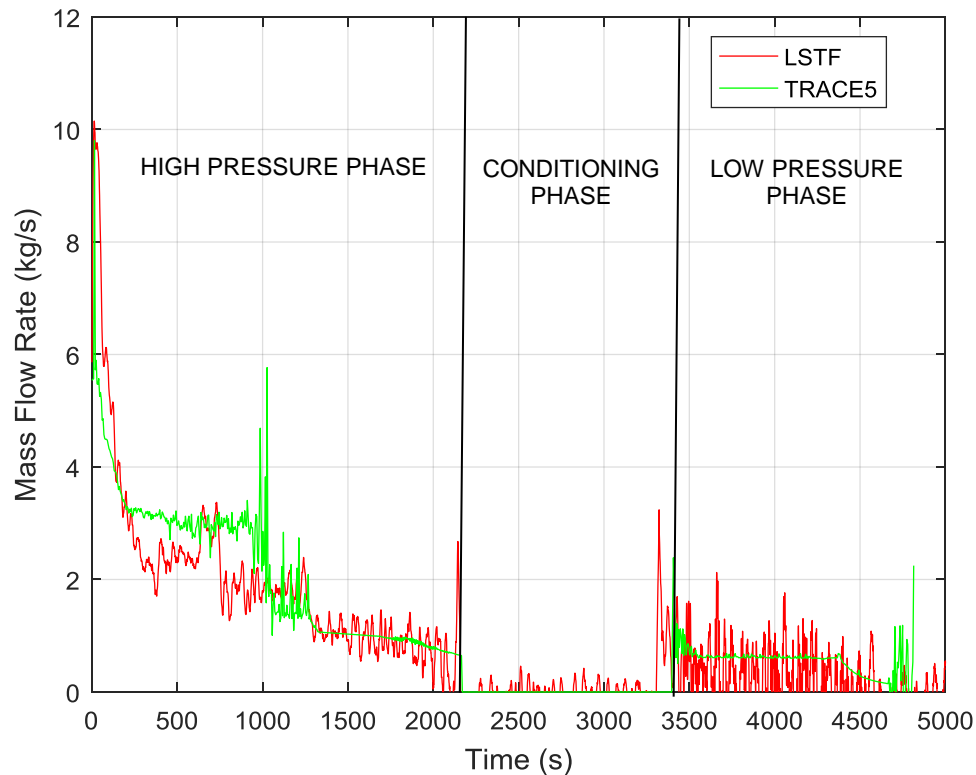


Figure 4 Break Mass Flow Rate

5.5 Primary Loop Mass Flows

Figures 5 and 6 show the primary mass flow rate in both loops. During the first seconds of the transient, the primary mass flow increases due to the higher angular speed of the pumps. Then, the primary mass flow rate in both loops decreases according to the pump coastdown.

The main discrepancies are found during the accumulator water injection. At 4500 s, the experimental primary mass flow rate in both loops are higher than the simulation results due to the accumulator water entrance in the cold legs. This effect has not been properly predicted by TRACE5.

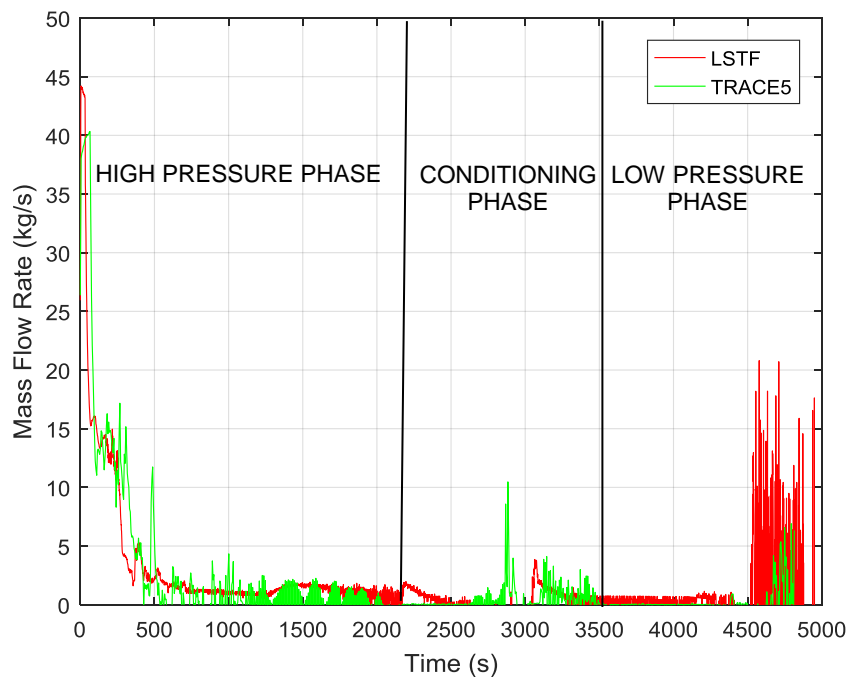


Figure 5 Primary Loop A Mass Flow Rate

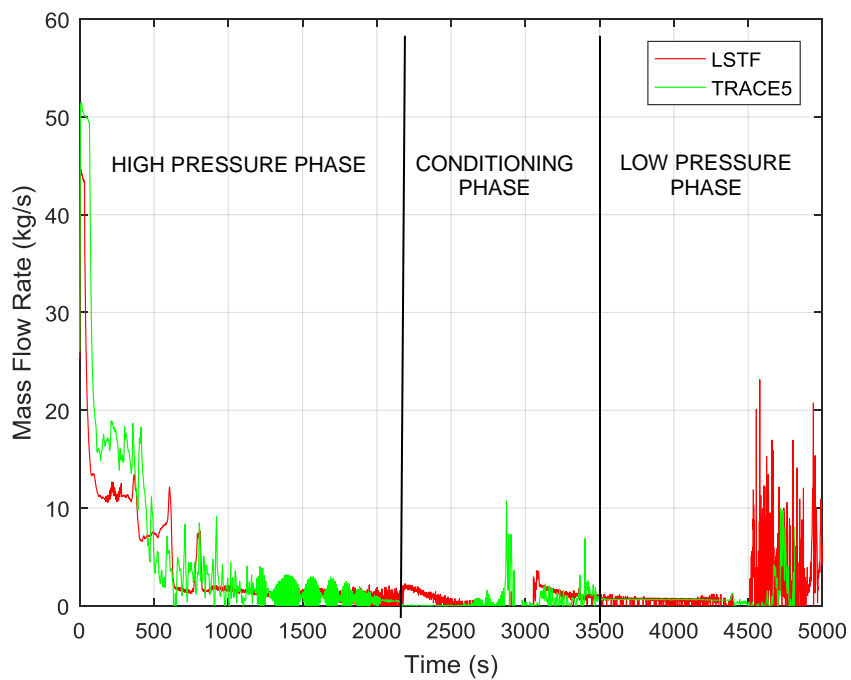


Figure 6 Primary Loop B Mass Flow Rate

5.6 Vessel Collapsed Liquid Levels

The Figures 7, 8 and 9 show a comparison between the collapsed liquid levels in the core, upper plenum and downcomer, respectively, obtained for both experimental and simulation results.

In the core liquid level, a significant drop starts due to the boil-off at about 1550 s, when the upper plenum is emptied. The core uncovering takes place after the primary pressure becomes lower than the secondary pressure. The collapsed liquid level continues to drop to about 1/3 of the active core length until 1870 s, even after the initiation of the high-pressure coolant injection into the PV upper plenum.

In the conditioning phase, the liquid level in the core and the upper plenum is recovered due to the high-pressure coolant injection. When the upper plenum reaches the middle level (at 2850 s), the HPI finishes.

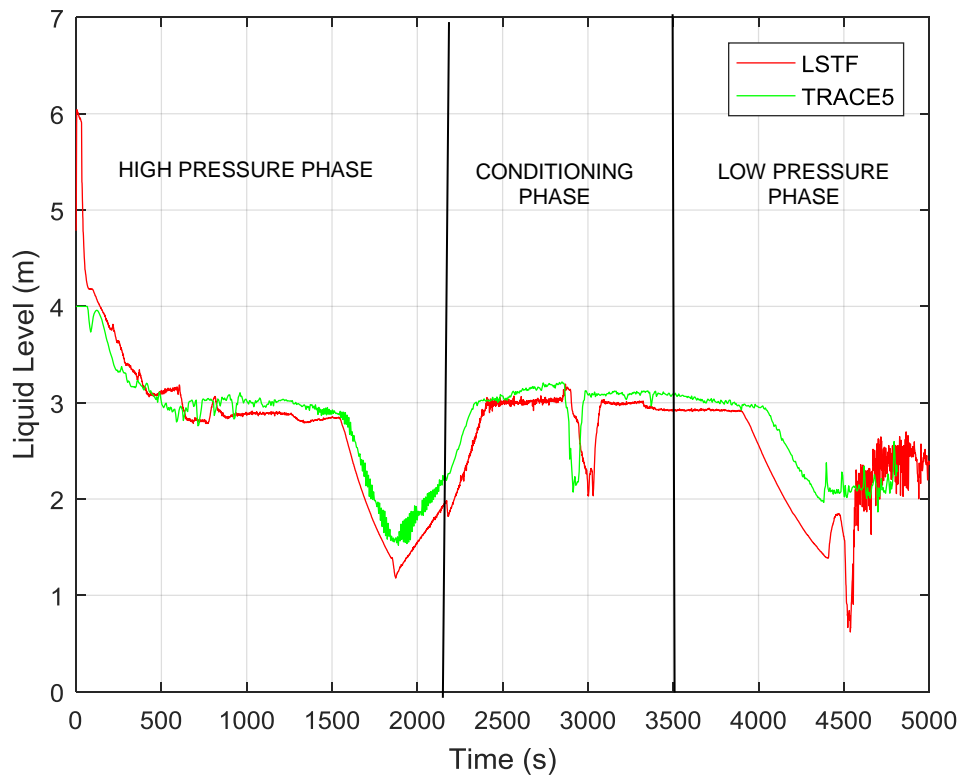


Figure 7 Core Collapsed Liquid Level

When the break valve is opened again at 3300s to start the low-pressure phase, the liquid level drops in the upper plenum and the core. The core liquid level begins to drop at about 3900 s, and the core uncovering is produced before the primary pressure becomes lower than the secondary pressure. The core liquid level is recovered following the primary depressurization.

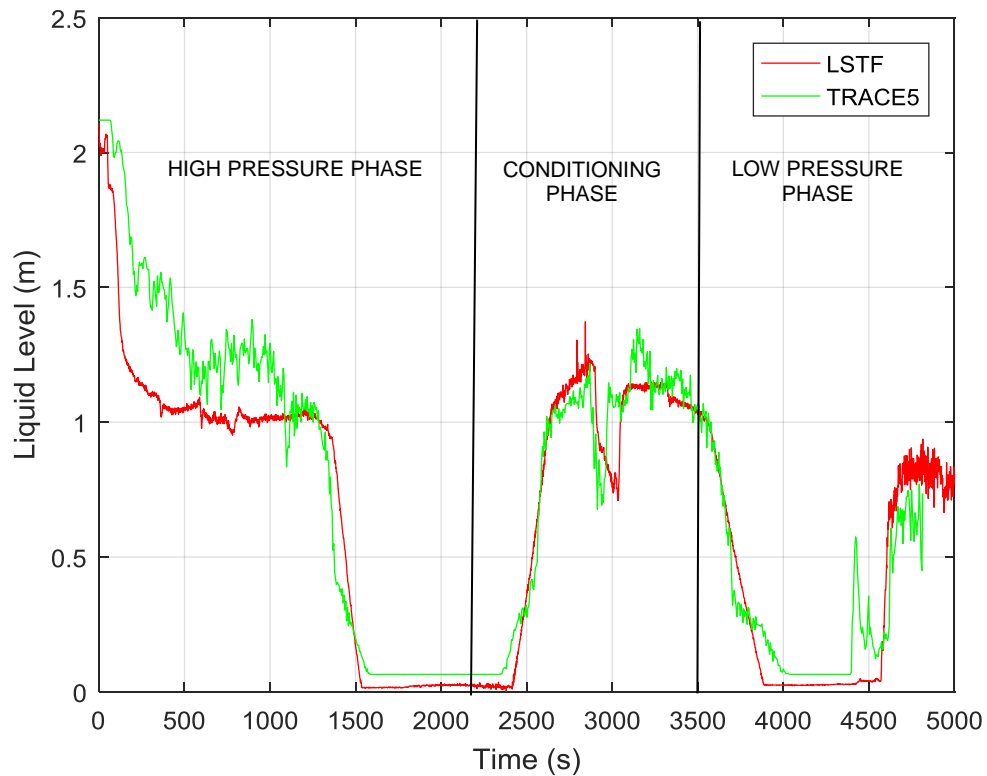


Figure 8 Upper Plenum Collapsed Liquid Level

Regarding the downcomer liquid level in the high pressure phase, it drops gradually up to 1800 s. It is recovered at 1910 s, after the initiation of the HPI into the PV upper plenum. In the conditioning phase, the temporary liquid level drop happens as in the upper plenum and the core due to the secondary depressurization.

In the low-pressure phase (after 3500 s), the liquid level drops following the core boil-off. The downcomer liquid level is steeply recovered at 4530 s due to the accumulator coolant injection. As it can be observed in Figure 9, some discrepancies appear during the first emptying of the downcomer, which is delayed in the simulation about 500 s.

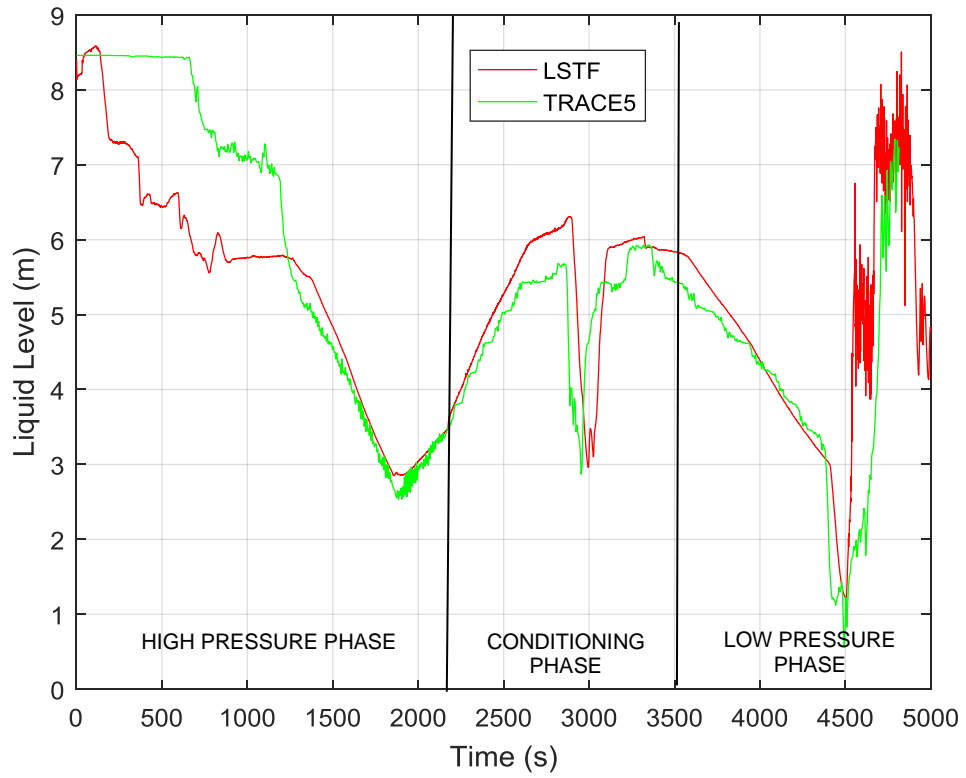


Figure 9 Downcomer Collapsed Liquid Level

5.7 Maximum Fuel Rod Surface and Core Exit Temperatures

Figure 10 shows a comparison between nine axial positions of a fuel rod. A HTSTR from the second radial ring has been chosen. The axial positions correspond to the nine axial levels in which is divided the core. The main discrepancies are observed during the second temperature excursion. TRACE5 does not reproduce the maximum value, obtaining a peak 100 K lower. In the high-pressure phase, the PCT reaches 750 K at 1840 s and the high pressure injection into the PV upper plenum is initiated.

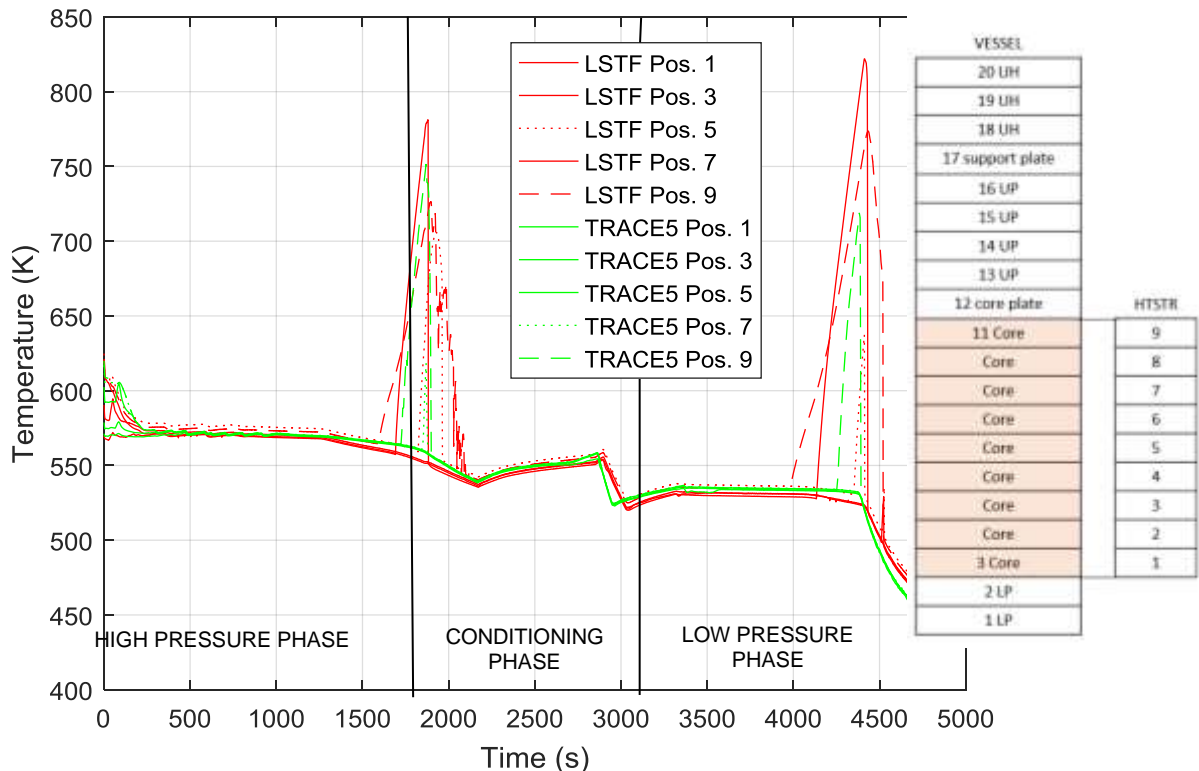


Figure 10 Fuel Rod Surface Temperatures at Different Axial Positions

In the experiments performed by the NEA Working Group on the Analysis and Management of Accidents [7], a significant difference between CET and PCT was observed in the measurements obtained in all the facilities. Thus, as the CET triggers the AM actions, but the safety variable normally followed in nuclear safety is the PCT, a more detailed study of both variables and the relation between them was suggested. Figure 11 shows the representation CET versus PCT. This figure allows clarifying the relation between CET measured by thermocouples and PCT during a hot leg SBLOCA. This relation allows obtaining the PCT that corresponds to a determined CET. The delay between the PCT and the CET excursions produces that the CET remains constant while the PCT increases to 600 K. However, in TRACE5 both excursions are initiated at the same time.

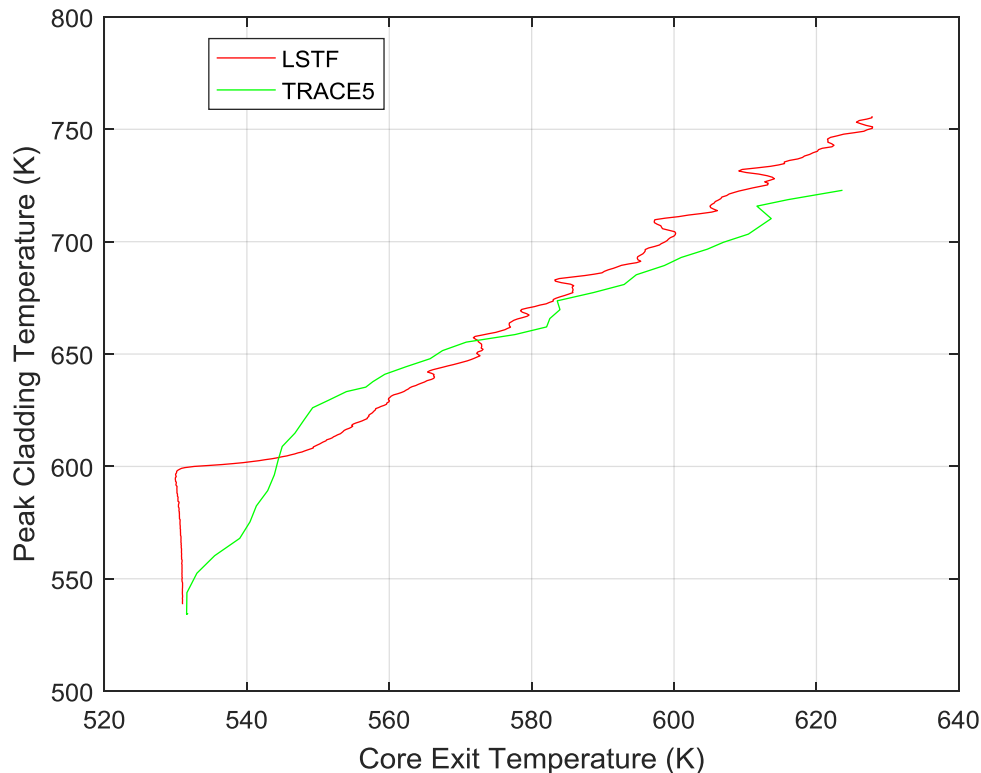


Figure 11 Maximum Fuel Rod Surface Temperature vs Core Exit Temperature

5.8 Hot and Cold Legs Liquid Levels

Figures 12 and 13 show the liquid level in both hot legs. As it can be seen, the liquid level is almost the same in both legs (intact and broken loop). In the high-pressure phase, the hot leg fluid becomes saturated at 53 s. The liquid level was kept at around 3/4 to 1/2 of the inner diameter until about 1310 s, when the steam break flow and primary pressure decreases. The hot leg becomes empty at about 1400 s, when the liquid level in the upper plenum begins to drop. In the conditioning phase, the hot leg liquid level is recovered at about 2640 s after the core reflooding and reaches the middle level. In the low-pressure phase, the liquid level starts to decrease just after the break valve open. The hot leg becomes empty at about 3600 s. The hot leg liquid level is recovered at 4530 s due to the accumulator injection. In high-and low-pressure phases, the fluid is kept saturated in the intact loop and superheated in the broken loop during the core uncovering. It suggests that the steam preferentially flows towards the break from the PV upper plenum while stagnates in the loop A, except during the SG depressurization. Figures 14 and 15 show the cold leg liquid levels. In loop A, the cold leg becomes empty at about 900 s, whereas in loop B it occurs at 1250 s. However, in the simulation both cold legs are empty at the same time (around 1250 s).

During the coolant injection by the accumulator and LPI systems, the liquid level is recovered in both loops. However, TRACE does not exactly reproduce the recovering of the liquid level in both cold legs, due to the rapid coolant discharge through the break from the accumulation injection.

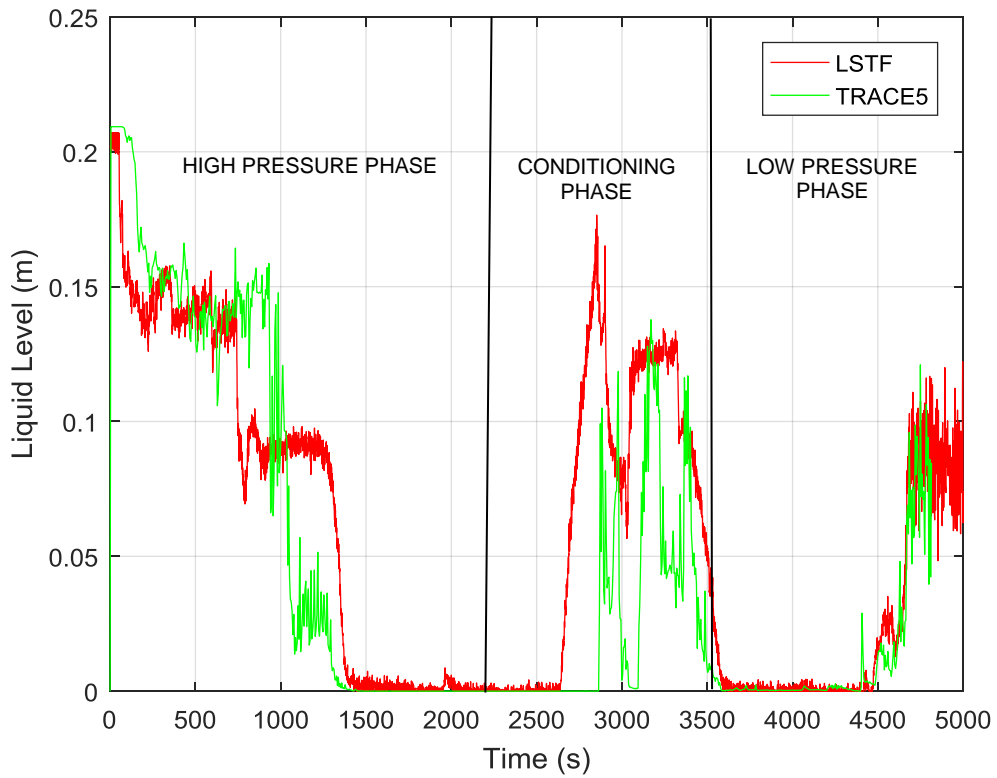


Figure 12 Collapsed Liquid Level in the Hot Leg A

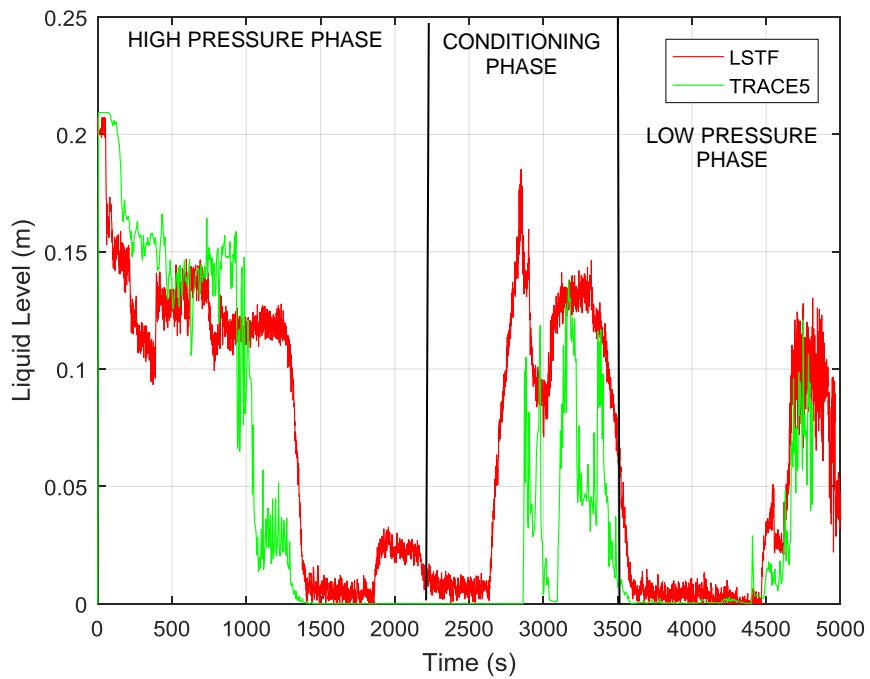


Figure 13 Collapsed Liquid Level in the Hot Leg B

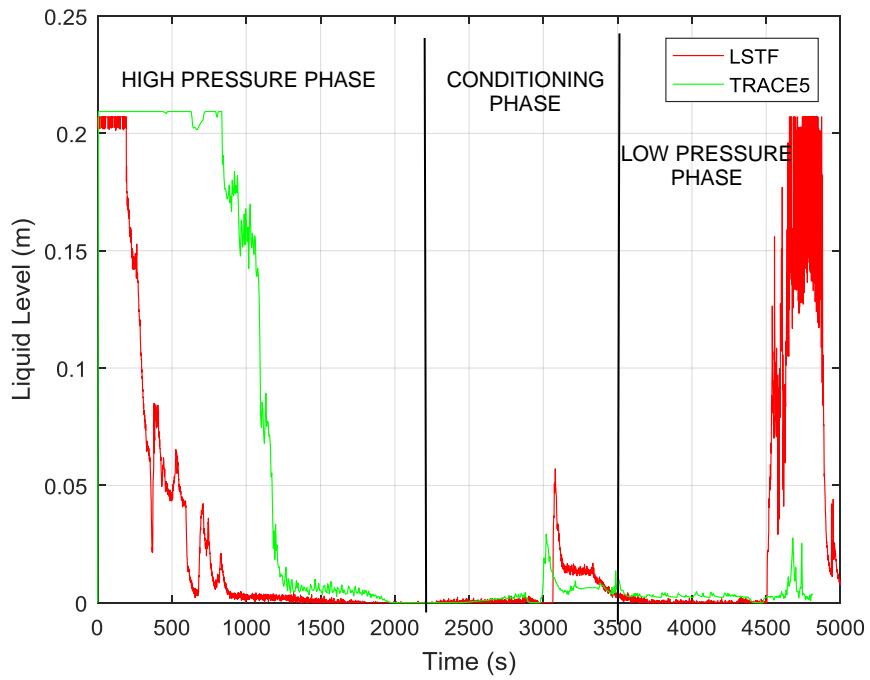


Figure 14 Collapsed Liquid Level in the Cold Leg A

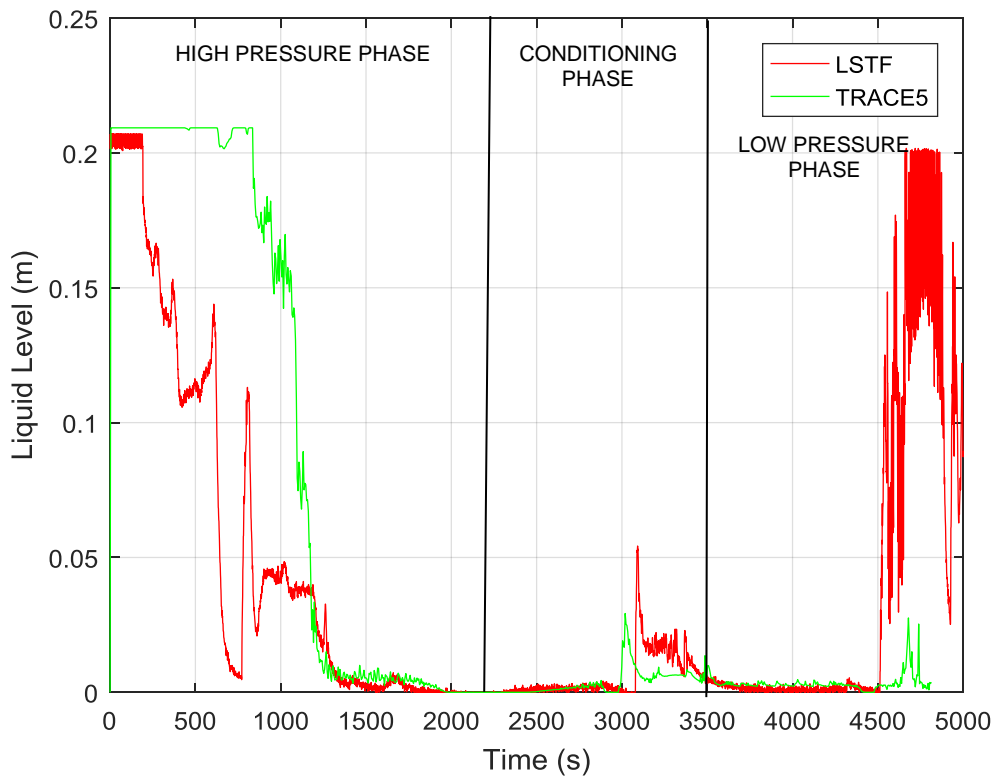


Figure 15 Collapsed Liquid Level in the Cold Leg B

5.9 Emergency Core Cooling Systems Mass Flow Rate

The HPI into the PV upper plenum is activated immediately after the maximum fuel rod surface temperature reaches 750 K (Figure 10). This HPI configuration is used to avoid thermal stratification occurring in the PV lower plenum. The coolant injection finishes at 2850 s, when the liquid level in the hot leg recovers the middle level. As it can be seen in Figure 16, where the HPI mass flow rates are shown, TRACE5 reproduces the HPI injection successfully.

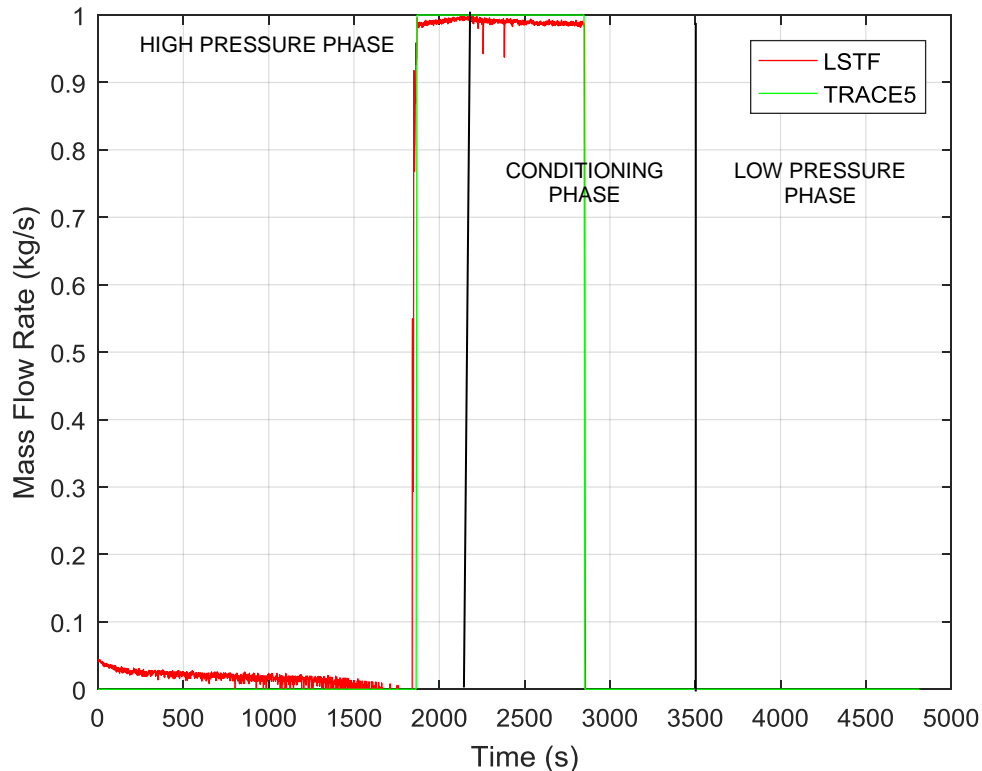


Figure 16 High Pressure Injection System Mass Flow Rate

Figure 17 shows the coolant injection flow rate from the Accumulator Injection System. As it can be seen, the simulated mass flow rate is lower than the experimental data, due to the different primary pressure drop. This fact could explain the differences in hot and cold legs refill.

The LPI system is activated in both loops at 5000 s. In the simulation, this event is advanced as it can be seen in Figure 18.

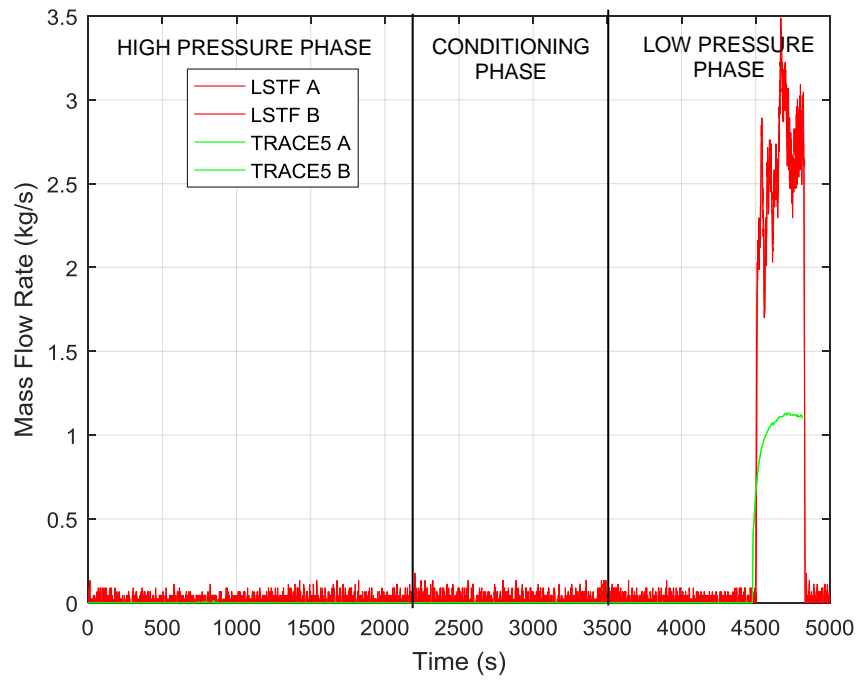


Figure 17 Accumulator Injection System Mass Flow Rate

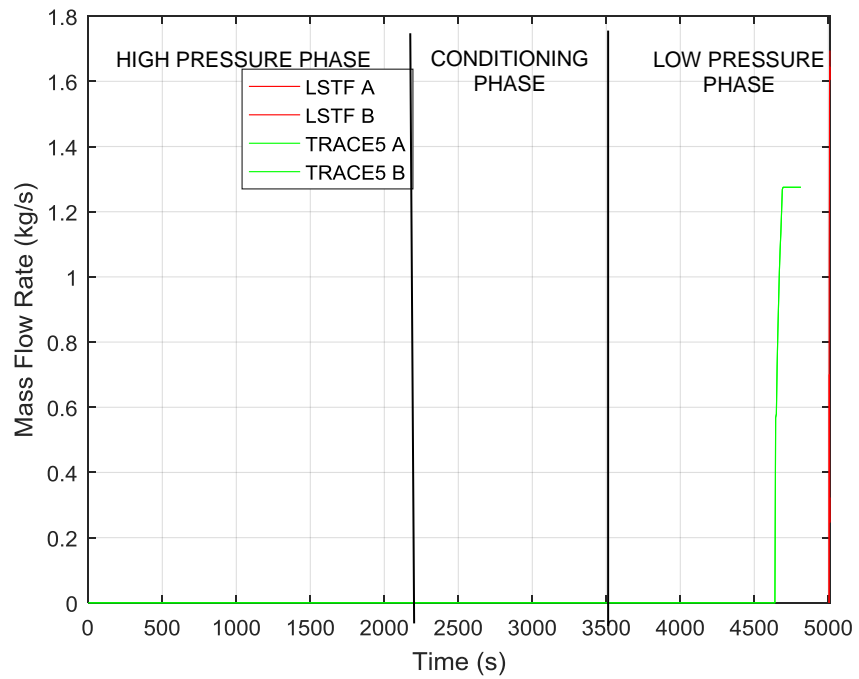


Figure 18 Low Pressure Injection System Mass Flow Rate

5.10 Core Power

Figure 19 shows the experimental and the simulated core power curves. The core power starts to decay at 50 s following the core power curve decay. The core power is manually changed to a constant value of 1.16 MW at 2215 s in the experiment and at 2500 s in the simulation. As it can be seen, the simulated core power curve has a good agreement with the experimental curve.

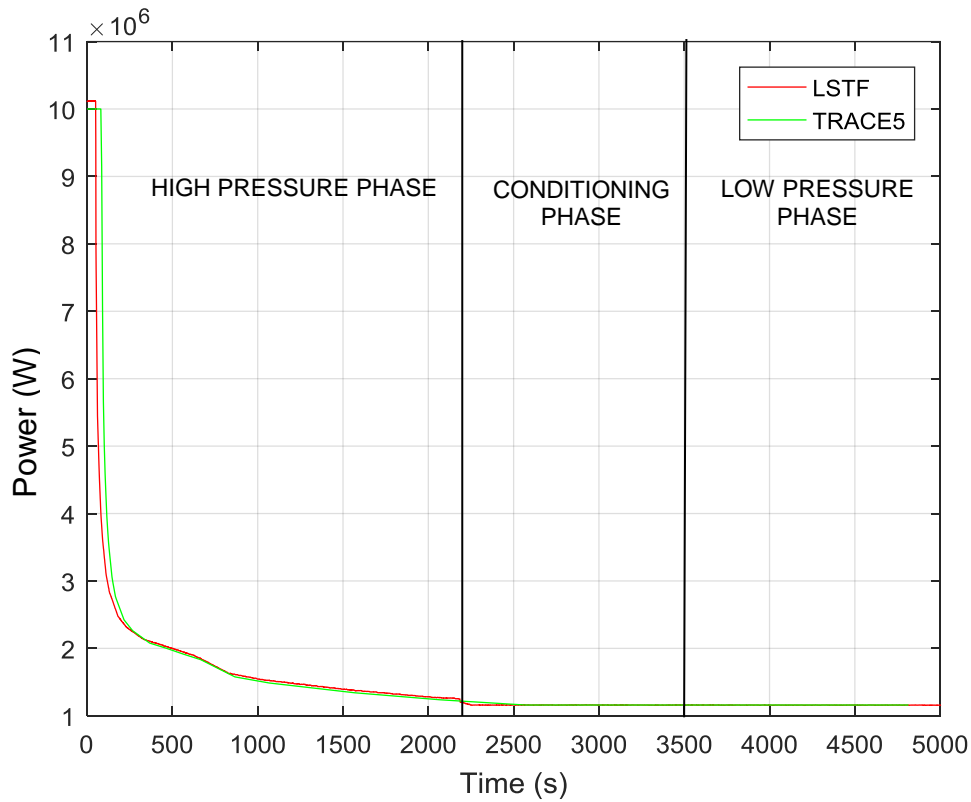


Figure 19 Core Power

5.11 Void Fraction

Figures 20, 21, 22, 23 and 24 show the void fraction achieved using the LSTF TRACE5 model during the transient, when important events happen. Figure 19 shows the void fraction in the LSTF at the initiation of the test. As it can be seen, primary and secondary sides are full of liquid at this time.

Figure 20 shows the void fraction when the PCT reaches 750 K and the HPI injection starts. At this time, the pressurizer is empty, and the liquid is located in the loop seals, accumulators, bottom of the PV and SGs. Figure 21 shows the void fraction when the primary pressure drops to 5 MPa and the break valve is closed. In this moment, the lower plenum of the PV, SG and AIS remain full of liquid, while the loop seals are almost empty. The situation when the second maximum of the PCT is reached is shown in Figure 22. SGs are empty while the loop seals

have some liquid. Finally, Figure 23 shows the void fraction at the end of the transient. As it can be seen, the SGs are almost empty and the accumulators have not been completely emptied.

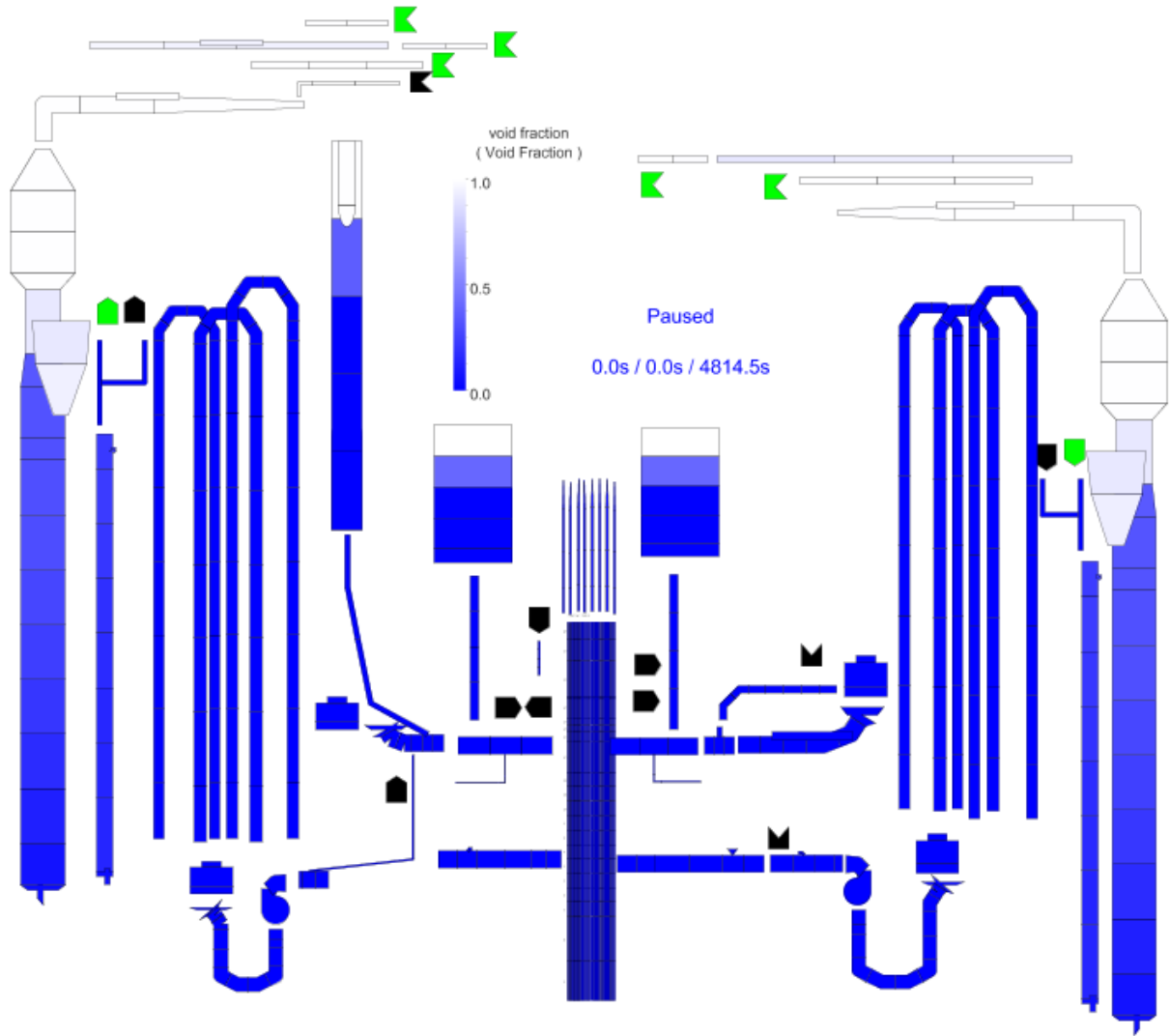


Figure 20 Void Fraction in the LSTF at 0 s

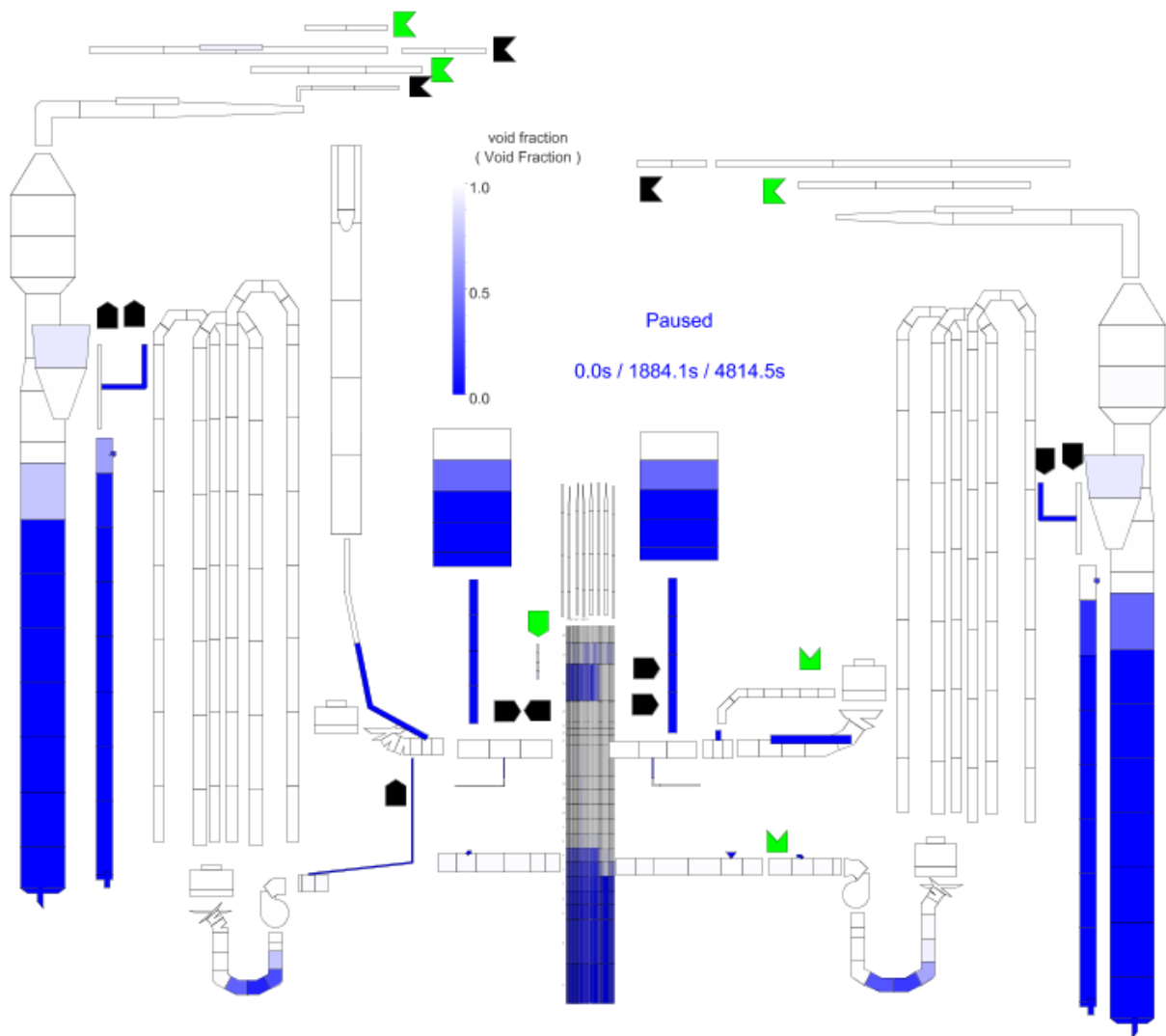


Figure 21 Void Fraction in the LSTF when PCT Reaches 750 K and HPI Starts

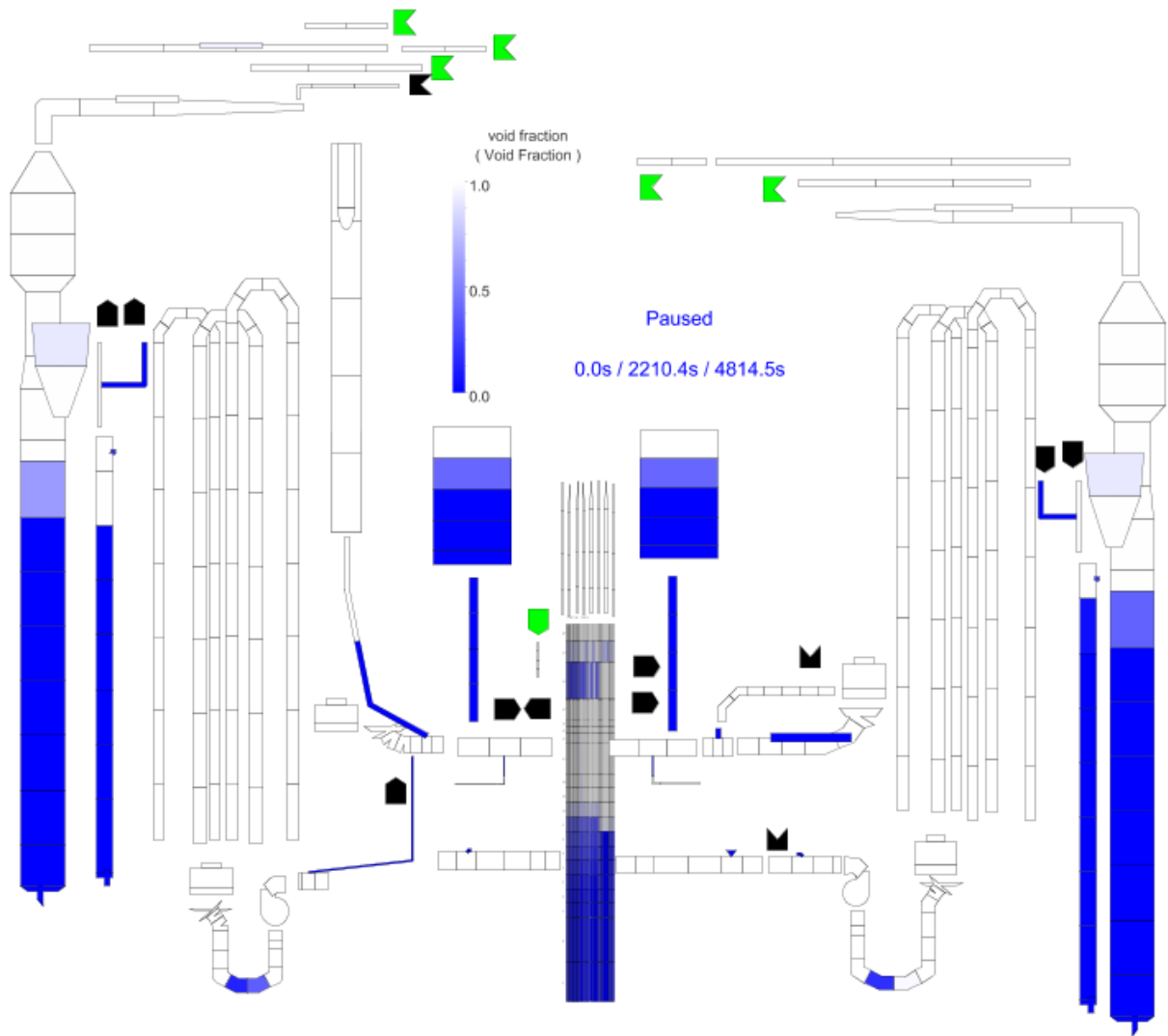


Figure 22 Void Fraction in the LSTF when Primary Pressure = 5 MPa

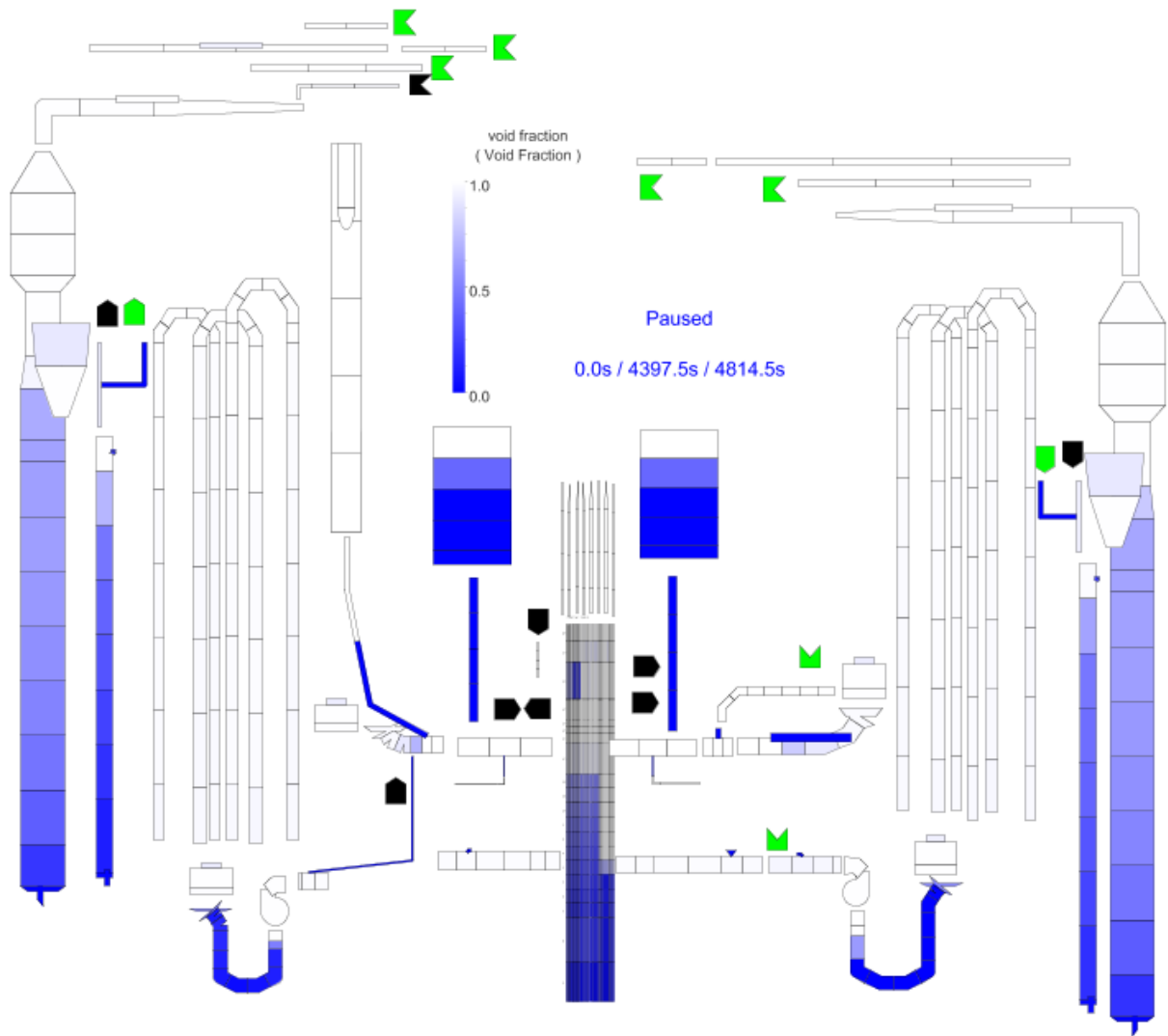


Figure 23 Void Fraction in the LSTF when Second PCT Excursion is Produced

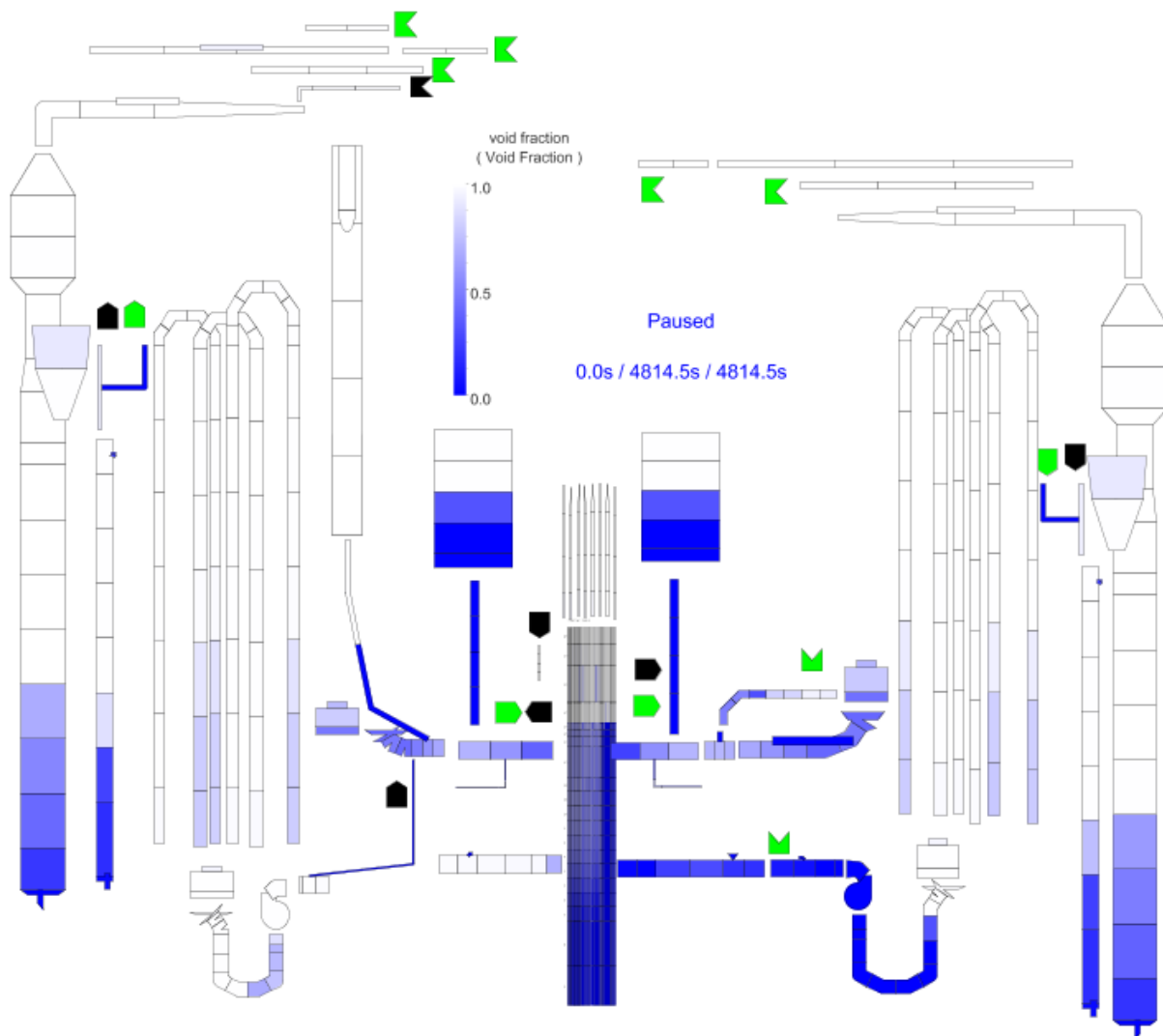


Figure 24 Void Fraction in the LSTF at the End of the Transient

6 CONCLUSIONS

Results show that TRACE5 can successfully reproduce all the phenomena produced in Test 3 OECD/NEA ROSA-2 Project (SB-HL-18 in JAEA) during the different transient phases: high-pressure, conditioning, and low-pressure. The main variables of the system present a good agreement in comparison to experimental data. System pressures, collapsed liquid levels in the PV, CET and PCT excursions are well reproduced. However, some discrepancies observed in the break mass flow rate could be attributed to the lack of a single-phase vapor coefficient in the choked flow model of TRACE5 patch 2. These differences can affect the mass flow rate through the hot and cold legs. Some discrepancies are also found in the maximum values reached during the second temperature excursions. However, these discrepancies do not affect the relation between the core exit temperature and the fuel rod surface temperature.

7 REFERENCES

1. Nuclear Regulatory Commission, Division of Risk Assessment and Special Projects. Office of Nuclear Regulatory Research. U. S Nuclear Regulatory Commission, TRACE V5.0. "Theory Manual. Field Equations, Solution Methods and Physical Models", Nuclear Regulatory Commission, U.S. (2007).
2. Nuclear Regulatory Commission, Division of Risk Assessment and Special Projects, Office of Nuclear Regulatory Research, TRACE V5.0. User's Manual. Volume 1: Input Specification, Nuclear Regulatory Commission, U. S (2007).
3. Thermohydraulic Safety Research Group, Nuclear Safety Research Center, Final Data Report of ROSA-2/LSTF Test 3 (Counterpart Test to PKL SB-HL-18), Japan Atomic Energy Agency, JAEA (2010).
4. The ROSA-V Group, ROSA-V Large Scale Test Facility (LSTF) System Description for the 3rd and 4th Simulated Fuel Assemblies, JAERI-Tech, Japan (2003).
5. Takeda, T., et al. Quick-look Data Report of OECD/NEA ROSA Project Test 6-1 (1.9% Pressure Vessel Upper Head Small Break LOCA Experiment). Japan Atomic Energy Agency, Private Communication. (2006).
6. Freixa J.; Manera A. Analysis of an RPV Upper Head SBLOCA at the ROSA Facility Using TRACE. Nuclear Engineering and Design, 240, pp. 1779-1788. (2010).
7. Toth, I., Prior, R., Sandervag, O., Umminger, K., Nakamura, H., Muellner, N., Cherubini, M., Del Nevo, A., D'Auria, F., Dreier, J., Alonso, J. R., Amri, A., "Core Exit Temperature (CET) in Accident Management of Nuclear Power Reactors", Nuclear Energy Agency, Committee on the Safety of Nuclear Installations, (2010).
8. Nakamura, H., Watanabe, T., Takeda, T., Maruyama, Y., Suzuki M., Overview of Recent Efforts through ROSA/LSTF Experiments. Nuclear Engineering and Technology 41(6), pp. 753-764, (2009).
9. Nuclear Regulatory Commission and Applied Programming Technology, Symbolic Nuclear Analysis Package (SNAP) (2012).
10. Freixa J.; Martnez-Quirogaa V.; Zerkakb O. and Revents F. 2015. Modelling Guidelines for Core Exit Temperature Simulations with System Codes. Nuclear Engineering and Design 286 (2015) 116-129.

BIBLIOGRAPHIC DATA SHEET

(See instructions on the reverse)

NUREG/IA-0504

2. TITLE AND SUBTITLE

Assessment of TRACE 5.0 Against ROSA-2 Test 3 Counterpart Test to PKL

3. DATE REPORT PUBLISHED

MONTH	YEAR
March	2019

4. FIN OR GRANT NUMBER

5. AUTHOR(S)

S. Gallardo, A. Querol, M. Lorduy, G. Verdu

6. TYPE OF REPORT

Technical

7. PERIOD COVERED (Inclusive Dates)

8. PERFORMING ORGANIZATION - NAME AND ADDRESS (If NRC, provide Division, Office or Region, U. S. Nuclear Regulatory Commission, and mailing address; if contractor, provide name and mailing address.)

Universitat Politècnica de València
Instituto Universitario de Seguridad Industrial, Radiofísica y Medioambiental
Camí de Vera s/n
46022 Valencia, SPAIN

9. SPONSORING ORGANIZATION - NAME AND ADDRESS (If NRC, type "Same as above", if contractor, provide NRC Division, Office or Region, U. S. Nuclear Regulatory Commission, and mailing address.)

Division of Systems Analysis
Office of Nuclear Regulatory Research
U.S. Nuclear Regulatory Commission
Washington, D.C. 20555-0001

10. SUPPLEMENTARY NOTES

K. Tien, NRC Project Manager

11. ABSTRACT (200 words or less)

The purpose of this work is to overview the results obtained by the simulation of the Counterpart Test 3 PKL-ROSA (SB-HL-18 in JAEA) in the Large Scale Test Facility (LSTF) using the thermal-hydraulic code TRACE5 patch 2. This experiment simulates a PWR hot leg Small Break Loss-Of-Coolant Accident (SBLOCA).

One of the main objectives of this test is to establish a relationship between the Core Exit Temperature (CET) measured by the thermocouples and the fuel rod surface temperature (Peak Cladding Temperature, PCT). The core exit thermocouples are used as an important indicator to start an accident management (AM) operator action by detecting core temperature excursion during reactor accidents. Test 3 provides experimental data to study the relation between CET and PCT and the time delay existing between them.

A detailed model of the LSTF and the control logic of the Test 3 have been simulated using TRACE5 patch 2. The main thermal hydraulic variables obtained with TRACE5 have been compared with experimental data. In general, the simulation results are able to reproduce the experimental behavior.

12. KEY WORDS/DESCRIPTORS (List words or phrases that will assist researchers in locating the report.)

Accident Management (AM)
Committee of the Safety of Nuclear Installations (CSNI)
Consejo de Seguridad Nuclear (Spanish Nuclear Regulatory Commission, CSN)
Core Exit Temperature (CET)
Large Scale Test Facility (LSTF)
High Pressure Charging Pump (PJ)
High Pressure Injection Pump (PL)
Intermediate Break Loss-of-Coolant-Accident (IBLOCA)

13. AVAILABILITY STATEMENT

unlimited

14. SECURITY CLASSIFICATION

(This Page)

unclassified

(This Report)

unclassified

15. NUMBER OF PAGES

16. PRICE



Federal Recycling Program



UNITED STATES
NUCLEAR REGULATORY COMMISSION
WASHINGTON, DC 20555-0001

OFFICIAL BUSINESS



nrc.gov

NUREG/IA-0504

Assessment of TRACE 5.0 Against ROSA-2 Test 3 Counterpart Test to PKL

March 2019